# Mutual Gravitational Capture as a Mechanism for Planetary Growth: An Alternative Hypothesis

José Mendes Damian
Independent Researcher, Brazil
Email: jmdamian@me.com | ORCID: 0009-0003-7726-1524
Linkedin: https://www.linkedin.com/in/jmdamian

**Declaration:**
This manuscript is a non-peer-reviewed preprint submitted to EarthArXiv.
The content has not been peer reviewed and represents the author's independent research.

# Mutual Gravitational Capture as a Mechanism for Planetary Growth: An Alternative Hypothesis


**ABSTRACT**

This study proposes a new hypothesis for the rapid growth of rocky planets through successive mutual gravitational capture events followed by planetary fusion. The model suggests that gravitational interactions between differentiated bodies with small mass differences can lead to collisions at velocities below the threshold required for full disruption, allowing fusion. The resulting planetary body, with mantle redistribution, internal reorganization, and potential orbital changes, would occupy an intermediate orbit.

The model predicts the formation of geological structures such as mountain belts, partial reassembly of the inner core, and mantle heterogeneities. Some of these signatures may be associated with the South Atlantic Magnetic Anomaly, mantle transition zones, subducted crust, and variations in biodiversity. During the process, part of the crust of the smaller body may temporarily form a supercontinent, which subsequently fragments into continental blocks.

The hypothesis provides an alternative to current paradigms and generates testable predictions for future investigations on the geodynamic, magnetic, and orbital evolution of Earth and other bodies in the Solar System.



Keywords: mountain belts, continental movement, mass extinctions, core and mantle heterogeneities, tectonics.


**Word Count: 8,960**

## 1. Introduction

This study analyzes Mutual Gravitational Capture (MGC), which occurs within the limits of the Hill sphere, a region where the attraction between two bodies exceeds external forces,

such as that of the Sun. The model investigates two main scenarios: (i) interactions between bodies with small mass ratio differences, whose orbital velocity vectors are aligned, resulting in approach and orbital convergence with an impact velocity mainly determined by mutual gravity; (ii) past conditions in which interactions between bodies with large mass ratio differences led to satellite capture or ejection. Under certain circumstances, a collision due to Mutual Gravitational Capture results in planetary coupling (MGC-PC), allowing the formation of a new celestial body, preserving pre-existing geological structures and leaving long-lasting multidisciplinary evidence on various scales.

Each MGC-PC event can lead to rapid and significant growth, with the possibility of mass doubling depending on the mass ratio between the bodies. The convergence of multidisciplinary data suggests that the MGC model may represent a relevant additional mechanism to existing models of planetary evolution, especially in contexts involving internal reorganization and orbital changes.

Classic models predict continuous growth through accretion and collisions [1], while others propose recurrent planetesimal formation, preserving volatile and isotopic diversity [2]. Models such as Giant Impact and Hit-and-Run explain discrete events, such as the formation of the Moon [3–4]. It is also noted that the fate of post-impact metals depends on the thermal state of the target body [5].

Morbidelli et al. [6] attribute Uranus's extreme axial tilt and the prograde rotation of its regular satellites to successive giant impacts. The causes and timing of the K–Pg extinction event remain a challenge for current models [7–9].

The limitations of current models and the search for alternative approaches have been highlighted by several authors. Bizzarro et al. [10] propose a rapid accretion model that preserves isotopic signatures. Crossley et al. [11] demonstrate that sulfide-rich cores can form in oxidized bodies without the need for extensive silicate melting. Ipatov [12], in turn, emphasizes the importance of migration and collisions as structuring mechanisms in the late evolution of planets and satellites.

Many models describe celestial bodies reaching their current configurations as if they were already nearly formed. However, close attention to the stage following initial accretion, involving collisions between differentiated and undifferentiated bodies, enables significant advances in interpreting observable evidence. Mergers between differentiated bodies represent this subsequent evolutionary stage, with direct implications for internal dynamics, magnetic fields, crustal structure, and even the evolution of biological systems.

In addition to engaging with the models discussed above, the MGC hypothesis may also provide meaningful contributions to specific aspects of planetary evolution. It incorporates collisions as structuring mechanisms in the evolutionary process, aligning with models that emphasize gentle instabilities, orbital migration, and systemic reconfigurations (Raymond et al. [13,14]). This perspective also helps explain the preservation of deep structural heterogeneities, in line with evidence for partial mergers discussed by Asphaug [15]. Furthermore, it allows for the reinterpretation of persistent magnetic anomalies as possible signatures of deep reorganizations at the core–mantle boundary, considering the sensitivity of the geodynamo to heat flow variations at the CMB, as highlighted by Biggin et al. [16] and Dannberg et al. [17].

In this manuscript, we propose a unified physical mechanism, derived from a systemic analysis of data gathered from various disciplines, aimed at explaining the complex cyclical processes that govern planetary evolution. The article is structured logically and progressively, through data, hypotheses, and interdisciplinary connections, culminating in a model that is still under development. With this model, we seek to reinterpret the multidisciplinary evidence referenced herein, acknowledging its validity and the conclusions currently accepted.

We recognize that, in interpreting the referenced studies individually, especially those from highly specialized fields, some inaccuracies may have occurred regarding the authors' original intentions. Nevertheless, we believe that many of these works address aspects potentially compatible with the proposed model. It is, therefore, a model open to continuous revision and an open invitation to constructive engagement.

## 2. Methodology

Two celestial bodies orbiting their star can interact gravitationally, resulting in a Mutual Gravitational Capture (MGC), which may lead to the following main outcomes: (i) the fusion of differentiated bodies through planetary coupling (MGC-PC); (ii) the orbital capture of satellites (MGC-SC); (iii) the ejection of smaller bodies (MGC-CE); or (iv) the formation of bilobed structures.

Genda & Abe [18] state: "*Terrestrial planets formed through gravitational accretion of a large number of planetary bodies (called planetesimals). The final stage of the accretion involved giant impacts between Mars-sized bodies*[4–7]*, and it was during this stage that the primordial atmosphere of the Earth was significantly modified*[8–10]*."* This statement opens

the way for the hypothesis that such events may also have occurred on Venus and Earth, as these are the only two inner planets with greater mass than Mars.

The focus of this study (MGC-PC) is primarily to analyze the enduring morphological signatures, the dynamics of the merger, and the resulting orbital effects, considering that collisions between differentiated bodies were common in the evolutionary history of the inner Solar System.

### 2.1. Theoretical Foundations of Mutual Gravitational Capture (MGC)

MGC occurs when two bodies enter one another's Hill sphere, and the gravitational attraction between them exceeds external influences, such as that of the Sun. From that point on, mutual gravity may gradually reduce the distance between them and their orbital velocity difference. In such cases, the relative approach velocity increases rapidly, ultimately resulting in a collision, with the impact velocity governed primarily by mutual gravitational attraction. The energy is dissipated mainly in the core and mantle, with significant contributions from crustal deformation and absorption by the atmosphere and oceans.

Based on these parameters, we adopted a conservative energy dissipation rate of 20%. Genda & Abe [18], although not providing a direct numerical value, demonstrate that oceans amplify atmospheric loss and rapidly convert impact energy into vapor, thereby increasing dissipation. Without explicitly stating the rate, Collins et al. [19] describe how impact energy is redistributed into heating, deformation, material ejection, and geochemical processes.

We also considered additional factors during the approach of the bodies, such as the convergence of orbital velocity vectors, which reduces the impact angle, and the progressive increase in tidal forces. Moreover, the mass ratio, the relative position of the bodies (i.e., whether the more massive body leads or follows), and other factors influence the orbital dynamics of the process.

***Critical velocity and planetary fusion:*** According to Genda et al. [20]: "$v_{(}cr_{)}/v_{(}esc_{)}$ *increases with decreasing impact angle or mass ratio, which means that collisions with low impact angles or low mass ratios tend to be merging events*" [20].

The authors indicate that successful merging occurs in collisions below the critical velocity, which can exceed the escape velocity of the system. Their model is summarized in an empirical formula to calculate the critical velocity:

$$\frac{v_{crit}}{v_{esc}} = c_1 \left(\frac{1-\gamma}{1+\gamma}\right)^{c_2} * [\cos(\theta)]^{c_3} + c_4 \left(\frac{1-\gamma}{1+\gamma}\right)^{c_5}$$

`

Here: γ is the mass ratio between the impactor and the target body ($\gamma = \frac{M_1}{M_2}$); θ is the impact angle and $c_1$ hrough $c_5$ are coefficients empirically derived by Genda et al. [20], based on hydrodynamic simulations.

In the absence of energy dissipation (η = 1) and initial relative velocity, the equations show that the head-on impact velocity corresponds to the escape velocity of the binary system ($v_{impact} = v_{esc}$):

$$v_{impact} = \sqrt{\eta\left(\frac{2GM_1}{r_{impact}} + \frac{2GM_2}{r_{impact}}\right)} \quad => \quad v_{impact} = \sqrt{\frac{2\eta G(M_1+M_2)}{r_{impact}}}$$

$$v_{esc} = \sqrt{\frac{2G(M_1+M_2)}{R_1+R_2}} \quad => \quad v_{esc} = \sqrt{\frac{2G(M_1+M_2)}{r_{impact}}}$$

Other key equations used in the theoretical framework include: Relative kinetic energy: $E_k = \frac{1}{2}\mu v_{rel}^2$, Hill limit (maximum distance of gravitational influence): $d_H = a\left(\frac{M}{3M_\odot}\right)^{1/3}$

Roche limit, which corresponds to the minimum distance at which non-rigid bodies with similar densities can approach each other without the near side of the smaller body breaking apart: $dR = 2.44R_M$.

Studies suggest that head-on impacts tend to be more destructive than low- to moderate-angle impacts (<45°) and that, depending on the mass ratio, they may result in either body fusion or grazing encounters [18, 20–25]. At higher angles (≥45°), hit-and-run events become common, with the impactor potentially escaping entirely in collisions with θ > 60°, as supported by several recent studies [23–25].

Denman et al. [22] demonstrate that head-on collisions between super-Earths are favored at low angles and low impact velocities, allowing for complete merging and the formation of a single planet. The authors further state that in such collisions, the cores of the two planets meet and combine at the gravitational center of the new body, forming a unified core. They conclude that part of the mantle may be ejected, while the remaining material redistributes around the combined core.

Canup [26] indicates that oblique impacts between nearly formed bodies can generate stable orbital disks, such as the one that may have given rise to the Moon, even without complete merging or total destruction. Additional studies suggest that moderate collisions

may lead to partial mergers and bilobed structures in undifferentiated bodies, such as certain asteroids and comets [27–29].

Raymond et al. [13] indicate that it was common for protoplanets, during this migration, to adjust their orbits and temporarily enter mutual resonances (such as 2:1 or 3:2) or to share nearby orbits, establishing a transient co-orbital regime. These dynamic conditions significantly increase the interaction time between massive bodies, favoring eventual collisions at controlled velocities.

### 2.2. Hypothesis and Modeling

Complementing studies that assume preexisting impact velocities, this model proposes a specific physical mechanism responsible for the collision velocities: mutual gravitational attraction between bodies in nearby orbits. In the context of the MGC-PC hypothesis, the small difference in orbital velocity and the approach driven by mutual gravitational attraction result in an impact velocity that is naturally regulated by the total mass of the system, favoring merger regimes such as those described by Genda et al. [20] and Denman et al. [22]. Thus, the modeling focuses on MGC-PC-type outcomes, in which coalescence between the bodies is physically feasible and orbitally favored, without requiring high initial velocities or destructive impacts. The table below summarizes three modeled scenarios used to assess collision viability, mass merging, and resulting morphological signatures:

| Scenario | Initial Configuration | Main Dynamics | Typical Outcome |
|---|---|---|---|
| (i) External | Outer body slower behind (chaser) | Outer body pulled inward, inner body pulled outward, with favorable rotation | Near-frontal angle, impact velocities near critical threshold |
| (ii) Internal | Inner body faster ahead (chaser) | Same as scenario (i), with opposite rotation | Similar to external, with opposite rotation |
| (iii) Direct | Orbital velocities and trajectories | High-energy collisions, material dispersal | Impacts with combined orbital and gravitational velocity |

*Scenario III will not be modeled, as it involves collisions driven by pre-existing orbital trajectories, without convergence governed by mutual gravitational attraction — a central condition of the MGC-PC model.*

***Scenario I:*** A collision occurs with the impactor on an outer orbit and with a near-zero difference in orbital velocity between the bodies. The bodies follow nearby elliptical orbits, so mutual gravitational attraction gradually aligns their direction and orbital velocity vectors, resulting in an impact angle tending toward head-on. This results in an impact angle tending toward frontal. The impact increases the total angular momentum, intensifying the rotation of the new planet. The resulting mass tends to follow the average direction of the orbital vectors of the colliding bodies, favoring coalescence and reducing dispersion.

***Scenario II:*** An impact on the inner side, under the same conditions as Scenario I, but with an impact vector opposite to the rotation, subtracting angular momentum. This may cause a deceleration or even a reversal of rotation.

The order of approach, that is, which body leads based on the mass ratio, influences the relative impact velocity, while the impact point determines the resulting obliquity. Different combinations of planetary rotations can produce complex effects. The modeled process is summarized in the diagram (Figure 2), which presents the stages from orbital approach to structural reorganization of the planet.

### 2.3. Application of the Model to the Formation of the Earth

Earth was chosen as the model due to its greater mass among the inner planets and the availability of multidisciplinary evidence for both the approach and merger phases. The model considers:

(i) Variable mass proportions between planetary bodies: Mass ratios between 40% and 60% of Earth's current mass should be considered, representing the smaller and larger bodies, respectively;

(ii) Gradual orbital convergence, with a decreasing orbital velocity difference between the planets, tending toward zero;

(iii) Relative impact velocity calculated based exclusively on mutual gravitational attraction, initially disregarding the small orbital velocity difference at the moment of collision;

(iv) Impact angle: assumed to be zero, which reduces the critical velocity required (worst-case scenario for fusion), although a very low angle is expected due to the approach being governed almost exclusively by mutual gravitational attraction. This choice aims to test the lower limit of coalescence. It is acknowledged that moderate angles (~30° to ~45°) are more favorable for fusion, and that this is a conceptual simplification;

(v) However, it is acknowledged that this residual orbital difference and a moderate impact angle (up to ~45°) may exist and could be incorporated into future simulations without significantly altering the expected outcomes.

The planet's rotation and thermal dissipation were considered empirically, without structural deformation calculations, reflecting the conceptual nature of the model. Section

4.13 discusses the model's limitations and sensitivities, including the rationale behind the adopted dissipation rate.

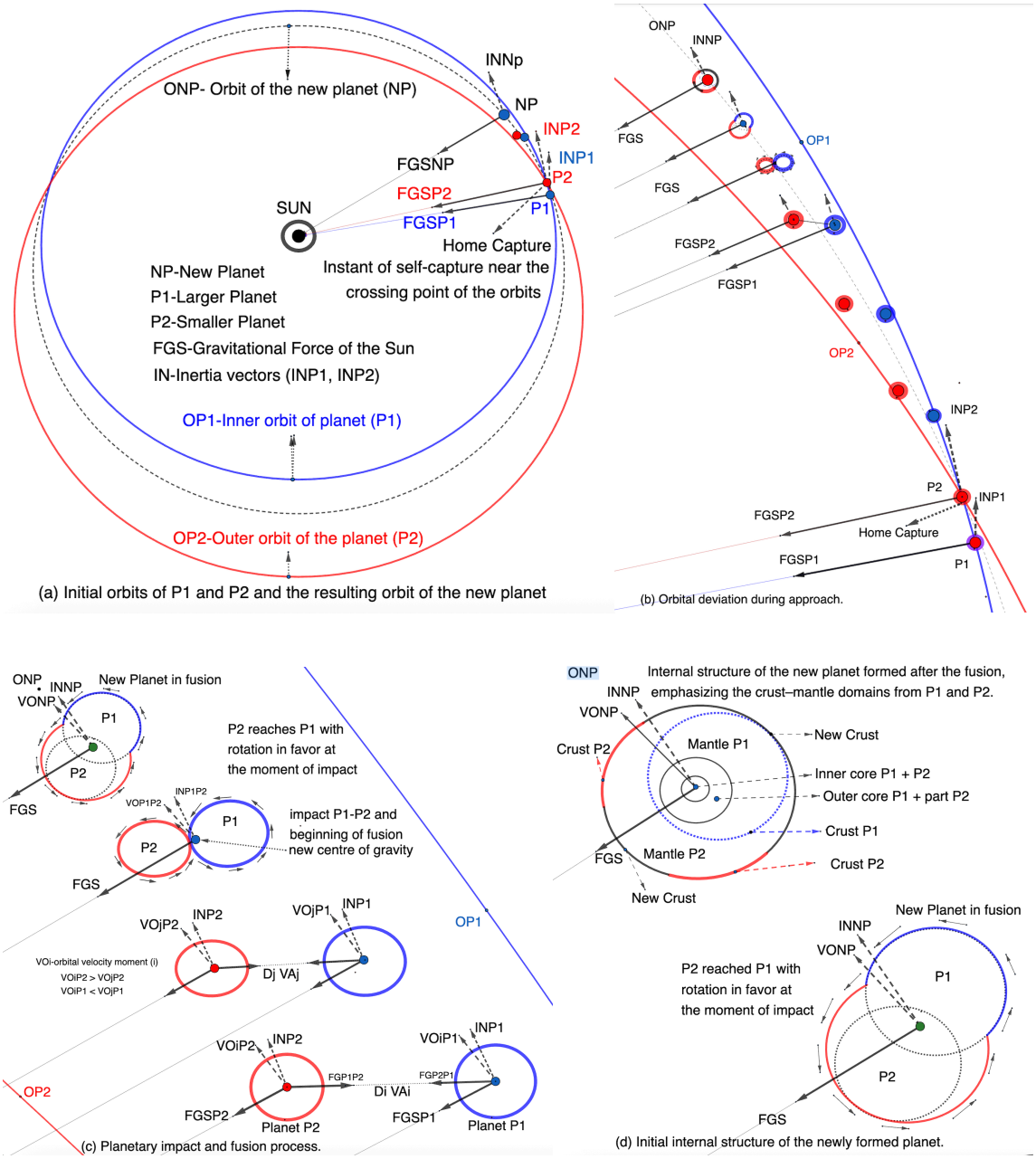


Figure 1 – Dynamic sequence of planetary merger.

# 3. Results: Parameter Analysis, Planetary Merging, and Morphological Modeling

We initially assess impact velocities in hypothetical MGC-PC events that may have led to the formation of the current inner planets of the Solar System.

## 3.1. Feasibility and Model Parameters

In this subsection, we assess the physical feasibility of the MGC-PC model based on orbital parameters, impact velocities, and stability tests. This process, although applied here to bodies smaller than Earth, shows partial similarities with the results of Denman et al. [22], obtained for collisions between super-Earths.

Among the inner planets, average orbital velocities range from 47.9 km/s (Mercury) to 17.9 km/s (Ceres). For modeling purposes, we considered head-on collisions between bodies with mass ratios between 40% and 60%, initially assuming that both had similar orbital velocities at the moment of impact. This is a significant simplification and represents a recognized limitation of the model, as orbital differences are expected in most real-world scenarios. However, we acknowledge that modest variations in relative velocity and impact angle are possible, depending on the mass ratio and which body leads the orbital trajectory during the approach.

***Impact Velocity Results:*** In our modeling, in the absence of initial relative velocity and dissipation, such collisions would generate impact velocities, caused by mutual gravitational attraction, ranging from 3.37 km/s (Mercury) to 8.79 km/s (Earth).

According to Genda et al. [20], the critical merging velocity for head-on collisions ($\theta = 0°$) is always greater than the escape velocity. For mass ratios close to 1, the critical velocity is greater than the system's escape velocity, that is, $v_{impact} \approx v_{esc} < v_{crit}$. This critical threshold may increase further as the mass ratio deviates from unity or as the impact angle becomes moderate. This margin supports the physical feasibility of planetary merging in a scenario that considers the worst case (head-on collision) and the best case (no difference in orbital velocity between the bodies immediately before impact). Thus, there is room for a moderate increase in impact angle and for small relative velocity differences at the moment of collision.

Using an energy dissipation of 20% or less, the estimated values remain below the critical threshold for catastrophic fragmentation, further supporting the viability of the model. Thus, with this dissipation, the estimated value remains well below the escape velocity, potentially varying slightly upward or downward depending on the impact geometry, energy dissipation, or collision angle.

These estimates are preliminary, based on conceptual simplifications, and require detailed numerical modeling to more accurately quantify fusion thresholds under varying impact conditions and compositions, as discussed in Section 4.13 – Limitations.

***Stability and Sensitivity Tests:*** Figure 4 presents a simulation of a complete cycle of the MGC-PC model, involving successive planetary fusion events and showing stepwise growth of mass, surface area, and gravitational acceleration, demonstrating the model's internal consistency. Variations in the mass ratio between 40% and 60% result in nearly overlapping velocity curves, indicating stability even with significant differences between the bodies. For cases where the smaller planet's mass ranges from 40% to 48% of Earth's mass and densities from 90% to 95%, calculations indicate a reduction in gravitational acceleration between 22% and 31%, with a corresponding decrease in atmospheric pressure (54% to 39%), not accounting for additional atmospheric loss suggested by recent studies. Although no formal statistical uncertainties or error bars were applied, these results represent a sensitivity analysis that demonstrates the model's consistency within a plausible parameter range. Future studies, preferably using hydrodynamic simulations, may refine these limits and assess the conditions under which the MGC-PC hypothesis remains valid.

In the following sections, we analyze the morphological evolution of the resulting body (3.2), its internal structures (3.3), and supporting empirical evidence (3.4).

### 3.2. Approach phase to impact

Capture begins at some point within the Hill sphere, when the difference in orbital velocities between the two bodies starts to decrease, evolving into a planetary coupling event (MGC-PC). During the approach to impact, pre-existing satellites may be relocated, ejected, or absorbed by the resulting planetary mass.

***Approach and gravitational deformation:*** As the bodies draw closer, their gravitational centers shift forward and the bodies become deformed into ellipsoidal shapes. Tidal forces intensify, accelerating the relative approach velocity and uplifting the crusts. Upon reaching the Roche limit, the leading crust of the smaller planet ruptures, while its opposite face preserves ancient cratons with geological records. The proportion of preserved crust is a hypothesis to be tested through geochemical studies and low-velocity impact modeling.

From this point, loose materials such as water and atmosphere migrate toward the displaced center of gravity in the impact region. The pointed crust of the larger planet comes into contact with the ruptured leading face of the smaller planet, possibly striking the mantle directly, which may be surrounded by oceanic waters. This configuration results from the ellipsoidal deformation caused by differential gravity, as predicted by the Roche limit.

According to the Borsuk–Ulam theorem, on any sphere there exist two opposite points sharing a common property. This symmetry may provide a potential mathematical basis to interpret crustal weakening observed on the side opposite the impact. The application of this concept is exploratory and remains subject to future validation.

Genda and Abe [18] show that terrestrial planets formed through the accretion of planetesimals, giving rise to dozens of Mars-sized protoplanets that collided with each other. These impacts generate shock waves that travel through the planet and affect the antipodal region of the impact site. They estimate that collisions between similar-sized bodies can result in up to 30% atmospheric loss and, for modeling purposes, assumed that all protoplanets near Earth's orbit possessed oceans during this phase.

The collision generates an asymmetric mass with a displaced center of gravity, initially located near the point of contact (Figure 1c), but within the larger body. Although applied here to differentiated bodies, this configuration resembles the bilobate structures observed in comets and asteroids, such as 67P/Churyumov-Gerasimenko and 4179 Toutatis.

***Loose Material Dynamics:*** The displaced gravitational center redistributes loose materials, water, sediments, and gases, creating what we refer to here as a hydrobiological ring, a conceptual illustration used to describe the transient concentration of water at the impact interface. The intense displacement of water, vastly greater than megatsunamis, is recorded in the continental crust. This ring formation represents a plausible hypothesis, although still speculative, grounded in physicochemical analogies that warrant further validation.

As the merger progresses, the center of gravity shifts and the new mass tends toward sphericity. The larger planet becomes covered by a layer of the smaller body's mantle, mixed with its own liquid core. Between these layers, an asymmetric interface zone develops, with significantly greater depth on the opposite side (Figure 1(d)). In this zone, a large portion of the Hydrobiological Ring material accumulates, where reactions occur between the mantle, the crust, the water, and other ring components, including biological matter. Under high pressure, these elements are expected to generate structural heterogeneities, hydrogen, and hydrocarbons.

The remaining material from the ring is redistributed over the expanding surface, flowing through unstable terrains and filling depressions that give rise to oceans and basins. The transported materials accumulate in these basins, where they are rapidly buried by sediments, including mud.

Water undergoes intense evaporation, forming salt layers and other soluble mineral deposits in regions with exposed mantle, and its vapors mix with other gases and ashes. This process increases ocean temperatures, creating a warm and acidic marine environment, and also triggers intense and prolonged rainfall. If present in sufficient quantity, water cools the magma and supports the continuation of life; otherwise, it may result in an acidic atmosphere. The new environment will exhibit a distinct chemical composition and climate patterns, with an expanded surface that alters the hydrological balance and sea levels.

***Preserved and newly formed crust:*** Upon impact, the preserved crust of the smaller planet fragments into continental blocks that float atop the mantle of the larger planet. These blocks move in seemingly random and independent patterns, guided by gravitational and rotational flows, as if surfing a wave. This mantle initially spreads out, drawn toward the center of gravity, which shifts as the new planet becomes more spherical.

New surfaces emerge between the moving continents, formed by lighter materials from the mantle. Initially, materials denser than the upper crust but still lighter than those that will later rise come to the surface, creating elevated regions at the zones of separation, as if forming magmatic ridges.

During continental drift, the leading edges of the continental blocks push magma ahead of them, due to their smaller curvature relative to the planetary mass. As the blocks move apart, they develop fractures in decreasing scales of length and width, forming a network of progressively smaller microfractures that adjust their curvature to accommodate the new planetary volume. The first curvature adjustment raises continental topography, forces mantle upwelling and may result in the formation of mountain belts along the leading edges.

### 3.3. Formation and final structure of the new planet

After the merger, an adjustment phase begins to balance the thickness and composition of the internal layers. Less dense materials from the larger body tend to rise, while denser materials from the smaller body, including its core, migrate toward the system's center of mass.

The larger body becomes covered by a variably thick layer composed of material from the smaller body, forming an interface zone (Figure 1d). This layer thickens on the side opposite the impact, while the original crust of the larger planet may remain exposed at the impact site, depending on the volume of the secondary body.

The density and increasing internal pressure and temperature favor the migration of solid cores toward the center of mass. Initially, the inner core may consist of juxtaposed solid spheres that gradually fuse, or not, depending on pressure, temperature, and composition. During migration, a low-pressure zone forms, attracting part of the outer core of the smaller body, including water and volatiles. The remaining material from the smaller body's outer core mixes with the mantle of the larger planet, either homogeneously or heterogeneously.

As the system stabilizes, the surface solidifies, and new tectonic plates are expected to form. The internal layers restructure by density, establishing a new equilibrium for rotation rates, including possible differential rotation among the inner spheres if they do not merge.

This event also alters the orbit, axial tilt, and other planetary motions, influenced by the proportions of the merged masses, solar gravity, and the action of satellites. The precession of the equinoxes changes drastically, reflecting the new gravitational configuration and the absence of the previously nearby body.

The resulting surface combines three distinct regions: preserved crust fragmented into continental blocks, newly formed crust creating elongated basins between these blocks, and a large plain at the impact site, where part of the larger planet's crust may be exposed. This large plain will have a semicircular shape with elevated edges, resembling a shallow basin or crater, resulting from the displacement of the smaller body's mantle under the influence of gravity, rotation, and interaction with water. For bodies with similar densities, the preserved crust of the smaller planet may account for up to 32% of the new surface.

Assuming equal densities, the new planet would have approximately 160% of the surface area of the smaller planet. If about 50% of the smaller planet's crust is preserved and fragmented into continental blocks, the continental surface of the new planet would represent about one-third of its total area. The remainder would consist of new, lower-lying regions with exposed magma. One of these newly formed areas will likely include plains between the diverging continental blocks, while at the impact site, the configuration will depend on the volume ratio between the bodies. In the final moments, the expanding mantle, under the action of gravity, rotation, and water interaction, tends to stop moving. This may result in a semicircular region, large or small, where the larger planet's crust remains exposed, surrounded by elevated rims.

The fusion event induces extinctions due to widespread chaos in the habitat, where plants, aquatic ecosystems, certain niches, and resilient species have better chances of survival.

`

***Morphological signatures resulting from fusion:*** Figure 2 illustrates the stages of planetary coupling (MGC-PC), including ellipsoidal deformation, gravitational redistribution, and interaction between mantles and crusts, highlighting the role of relative masses and energy dissipation in the dynamics of fusion. Figure 3 shows the resulting morphological features, such as the impact plain, preserved migrating continental blocks, fracture zones, and magmatic ridges. These structures provide an empirical reference for evaluating the proposed model.

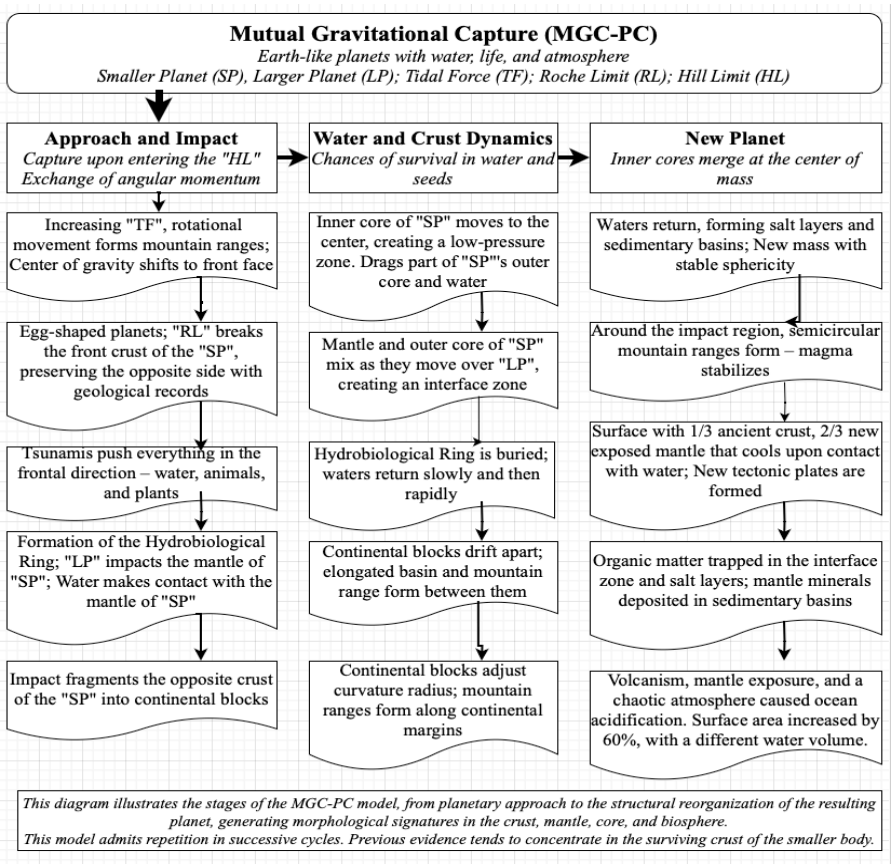


Figure 2 – Steps of the MGC-PC process resulting from Mutual Gravitational Capture (MGC).

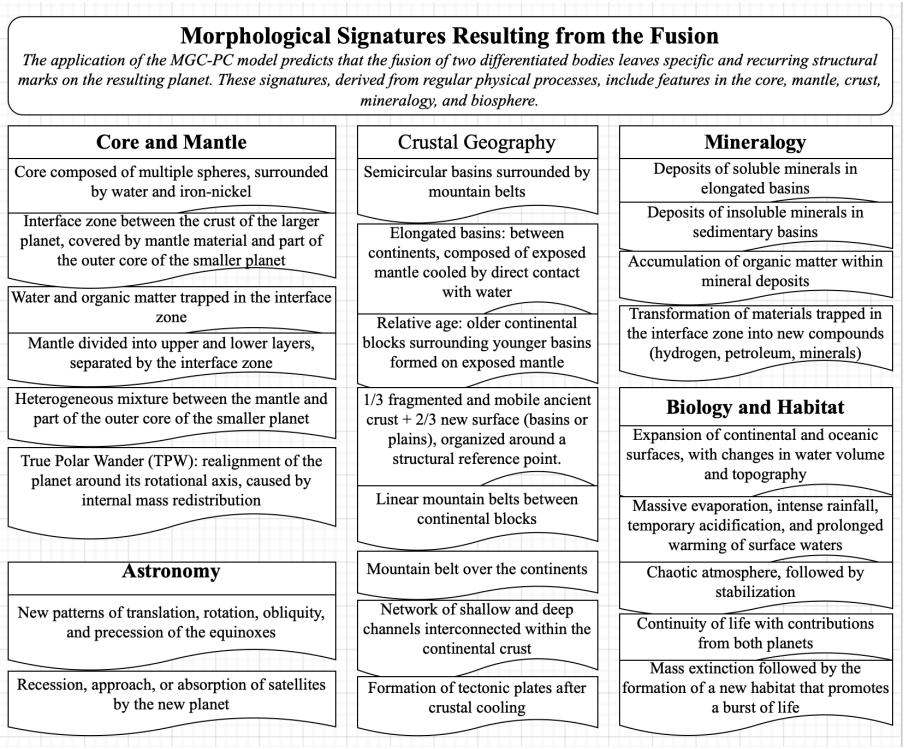


Figure 3 – Persistent morphological signatures generated by the MGC process.

## 4. Discussion

This velocity equals the escape velocity of the system but is reduced by energy dissipation, remaining below the critical fragmentation threshold proposed by Genda et al. [20], thus favoring complete fusion. For the inner planets, such velocities are significantly lower than their orbital velocities, the opposite of what occurs with more distant planets. This physical feasibility is also supported in the literature. Raymond et al. [13] observed that collisions between protoplanets in nearby orbits tend to occur at low velocities, favoring fusion.

Based on this framework, Sections 4.1 to 4.7 reassess empirical evidence in light of the MGC-PC hypothesis, with a focus on different fields within the geosciences:

- Geophysics and Geodynamics: mantle heterogeneities (ULVZs, LLSVPs, water-rich layers in the transition zone, hotspots, plumes, SAMA, Yellowstone), magnetic anomalies, growth and physical state of the inner core, and zircon records linked to deep geodynamic processes (sections 4.1 and 4.2);
- Structural Geology, Paleogeography, and Tectonics: mountain building, crustal fragmentation and reorganization, and the development of large intercontinental plains (sections 4.3 and 4.4);

- Geochemistry and Mineralogy: interaction between water and the mantle, involving the transport and accumulation of soluble and insoluble minerals in sedimentary basins, the formation of saline layers in internal oceans, and the entrapment of organic matter beneath the mantle or salt layers, later transformed into hydrocarbons (section 4.5);
- Paleontology and Evolution of Life: mass extinctions, biotic reorganizations, environmental impacts, and fossil records (sections 4.6 and 4.7).

In Sections 4.8 to 4.12, the focus shifts to astronomy and planetary sciences: the evolution of inner bodies, orbits, rotation, and implications for astrobiology, as well as for the formation of satellites and comets. The model is conceptually applied to planetary coupling cycles, deep geophysical and geochemical signatures, parallels on other planets, and contrasts with existing models.

Finally, Section 4.13 presents the methodological limitations and simplifications of the hypothesis.

### 4.1. Geophysics of the New Planet: Core and Magnetic Anomalies

The MGC-PC process proposes that the fusion of differentiated bodies reorganized the core, mantle, and crust, favoring the migration of multiple inner cores toward the new center of mass. This movement created low-pressure zones that attracted volatiles and viscous materials, including water.

This process may result in an inner core composed of several solid spheres surrounded by metallic liquids and volatiles, rotating independently in cases where the cores do not fully merge. However, this dynamic state may gradually evolve toward unified rotation as the body stabilizes its total angular momentum.

Seismological observations reveal physical heterogeneities, anisotropies, rotational variations, and structural changes in the shape and composition of the inner core [31–34], incompatible with the view of a single, homogeneous, and static body. He et al. [35] state: “The Earth's inner core (IC) is less dense than pure iron, indicating the presence of light elements within it. Silicon, sulfur, carbon, oxygen, and hydrogen have been suggested as possible candidates.”

Deuss [36] shows that the upper 60–80 km of the inner core appear isotropic, while the central region is anisotropic, with seismic waves propagating faster along the polar direction. Zhou et al. [37] show that the geomagnetic field was very weak around 565 Ma,

increasing rapidly after 550 Ma, coinciding with the probable growth of the inner core to ~50% of its current radius by 450 Ma.

The MGC-PC hypothesis suggests that, in addition to the inner core doubling in size with each successive event, internal pressure increases. This favors physicochemical interactions and the migration of dispersed iron in the mantle toward the center, contributing to the progressive growth of the inner core. Consequently, the inner core would consist of the original solid cores, supplemented by volatiles filling the spaces between these spheres. This approach provides a new physical basis for interpreting the observed heterogeneities, supporting the need to revise the conception of the inner core as a solid, homogeneous, and static body.

### 4.2. Geophysics of the new planet: mantle heterogeneity

The MGC-PC model suggests that the mantle of the smaller planet mixed with part of its outer core and spread over the larger planet. This process formed a layer that partially or almost completely covered its crust, possibly generating heterogeneities compatible with the seismic, geochemical, and thermal anomalies currently observed in Earth's mantle. Within these layers, an interface zone is established, significantly deeper on the side opposite the impact (Figure 1(d)). This zone may extend through the transition zone down to the Gutenberg discontinuity, trapping water, organic matter, and other volatiles capable of generating hydrogen and hydrocarbons under high pressure. Evidence of water retained in mantle minerals [38–41] and calcium-rich rocks below 300 km depth [42] is compatible with this scenario.

Hotspot regions [43] may represent a heterogeneous mixture of mantle material and the outer core, while the Yellowstone supervolcano, with its sulfurous waters and yellowish rocks [33], suggests a moderate mixing between the mantle and the outer core, the latter enriched in sulfur (Savage [30]).

During this process, the inner core of the smaller planet, initially displaced, migrates toward the new common gravitational center from the side opposite the impact location. Along this path, it may drag volatile materials, such as water and liquid iron-nickel. Part of this flow may form persistent compositional bubbles in the mantle, potentially linked to the South Atlantic Magnetic Anomaly (SAMA).

The buried crust, initially continuous, may fragment into blocks of different sizes (small, medium, or large), creating deep heterogeneities. Consequently, the crust of the larger planet became covered by mantle material through a process distinct from the

subduction described by plate tectonics, potentially explaining the formation of structures such as LLSVPs and ULVZs [16,17,45–49]. Internal mass redistributions associated with these processes may also have contributed to episodes of True Polar Wander (TPW). Vaes & van Hinsbergen [50] indicate that during TPW events, the crust and mantle move together relative to the rotation axis, causing all continents to shift simultaneously. These episodes occurred between 320–200 Ma and during the last 80 Ma. Van Hinsbergen et al. [51] show that major tectonic reorganizations, including the initiation of subduction, may be triggered by deep mantle plumes, without prior collisions or pre-existing convergent boundaries.

Additional studies support the hypothesis of crustal burial and mantle-core mixing during successive planetary fusion cycles. Dannberg et al. [17] indicate that thermal heterogeneities at the core-mantle boundary (CMB) evolve cyclically with the formation and breakup of supercontinents, generating deep structural anomalies that affect the planet's thermal and magnetic dynamics. Small zircon populations dated between 165 Ma and 2.5 Ga [52–54] and magnetic signatures preserved in iron-rich minerals within the transition zone [55] reinforce this scenario. Messling et al. [56] identified positive $\varepsilon^{100}$Ru anomalies and negative $\mu^{182}$W signatures in modern basalts from Hawaii, Greenland, Africa, and Germany, concluding that outer core material was incorporated into the deep mantle during the first ~60 million years of the Solar System.

Although individual explanations for these observations exist in the literature, the combined evidence aligns with the expected effects of MGC-PC events, which would redistribute crustal material, volatiles, and metals to different mantle depths.

### 4.3. Structural Geology, Paleogeography, and Tectonics: Orogenic Processes

Orogenic belts coincide with major geological events, such as mass extinctions and supercontinent fragmentation, and may serve as morphological markers of MGC-PC cycles (Section 4.8). Recent belts suggest an MGC-PC event occurred around 66 Ma, formed through four main mechanisms:

i. crustal uplift driven by tidal forces (Alpine-Himalayan Orogeny);
ii. magma release at the onset of continental breakup (Mid-Ocean Ridges);
iii. adjustment of the curvature radius along continental margins (Andean Belt);
iv. structures associated with the ancient subduction zone of the larger planet (Ring of Fire).

The model proposes that strong tidal forces during planetary approach, prior to reaching the Roche limit, uplifted the crust, forming the Alpine-Himalayan structure. Some authors describe its formation in four distinct phases within the last 66 Ma [57], while others place the main collision between ~55 and 50 Ma [58]. The Ring of Fire may represent the boundary of the ancient subduction zone of the larger planet, with its crust exposed within the perimeter of the ring.

Mid-ocean ridges may have resulted from the initial upwelling of lower-density magma, exposed during the early drift of continental blocks. The rapid uplift of the Andes, recorded as abrupt between 10 and 6 Ma [59], is consistent with the initial curvature adjustment proposed by the model.

### 4.4. Structural Geology, Paleogeography, and Tectonics: Crustal Restructuring and Geodynamic Implications

The crust of the new planet results from young surfaces formed by exposed magma, portions of the larger planet's crust, and blocks from the smaller planet's crust. The latter initially forms a temporary supercontinent, which subsequently fragments into continental blocks. On present-day Earth, the North Pacific may indicate the impact point of the final event, while the southern region of Africa, at the antipode, may reflect an area of weakened crust.

***Supercontinent cycle:*** Nance et al. [60, 61] suggest that the supercontinent cycle is associated with global tectonic reorganization involving changes in mantle flow, core dynamics, and climate, potentially triggering volcanism and large-scale environmental disturbances. They emphasize that current models assume a constant planetary surface and rely only on lateral forces, indicating the need for a more complex approach that incorporates deep crustal restructuring and non-conventional internal processes. Pastor-Galán et al. [62] link the formation and breakup of supercontinents to environmental changes and variations in Earth's magnetic field. Studies suggest that the assembly and breakup of Rodinia (~750 Ma) and Pannotia (~550 Ma) followed these patterns [60, 63].

In this context, the MGC-PC hypothesis offers an alternative framework: it proposes that the planetary surface may expand significantly after fusion events, with new continents forming and moving independently of conventional tectonic plates, potentially experiencing differential subsidence. This post-impact reorganization can be interpreted as a phenomenon analogous to True Polar Wander (TPW) [50]. In the context of the MGC-PC model, it results from the differential movement of the crust relative to the new planetary center after fusion, distinct from classical TPW, which is associated solely with internal mass redistributions.

Examples of subsidence include Greater Adria, which was almost entirely subducted and incorporated into the Alpine orogens [64], and Zealandia, a submerged and fragmented continent.

***Supercontinent reconstruction:*** The MGC-PC model suggests that, assuming equal densities and an idealized spherical shape, the new planet would have approximately one-third of its surface composed of preserved crust from the smaller planet—a value close to the current continental area of Earth (~29%). Retroactively reconstructing past continents is complex, as it depends on the volume of water present during each evolutionary stage of the smaller planet (see Section 4.10). Ancient cratons do not necessarily imply emergent landmasses. The reconstruction process may involve removing low-lying regions, resizing the planet until preserved blocks cover about 50% of the surface, disregarding the opposite hemisphere as ancient oceanic basins, and repeating the procedure cycle by cycle. For greater accuracy, it is advisable to use the oldest cratons as paleogeographic anchors and to consider major regional geological structures, particularly orogenic belts.

### 4.5. Geochemistry and Mineralogy: Petroleum and Mineral Reserves

The MGC-PC hypothesis proposes that, during planetary fusion events, large volumes of water interacted abruptly with the mantle and the outer core of the smaller planet, burying part of this water along with organic matter under extreme temperature and pressure conditions.

Hydrocarbons: Organic matter and water may have been buried in deep, high-temperature zones at the interface between the colliding bodies (Figure 1(d)) or near the surface beneath layers of salt acting as natural catalysts. These environments could have generated hydrocarbons both in the mantle and in shallow regions, consistent with biogenic and abiogenic theories [65–67]. Current petroleum reserves, often located in former marine regions [68, 69], may reflect these processes. Höök et al. [66] examined both models, highlighting stronger empirical support for a biogenic origin.

Minerals: MGC-PC events may have promoted direct contact between ocean water and exposed mantle, dissolving metals and transporting them to continental basins or depositing them on ocean floors. Over time, these metals became fixed in continental regions or in ferromanganese nodules on the seafloor. Evidence described in [70–73] explains the presence of metals in seawater and continental deposits, even in locations without signs of volcanism or hydrothermal activity, which were once oceanic floors. In continental basins, metals were rapidly covered by sediments or mud, while soluble minerals were fixed more

slowly through chemical or biological processes. Beneath these deposits lies the preserved crust of the smaller planet.

### 4.6. Paleontology and Evolution of Life: Biological Evolution, Extinctions, and Dinosaurs

Mass extinctions coincide with abrupt changes in climate, sea level, and biodiversity crises [8, 9, 74–77]. The Cambrian Explosion coincided with rising $O_2$ levels [78] and the breakup of Pannotia [60, 63]. Diversification and extinction events occurred rapidly, with complex and geographically widespread patterns in specific periods, lacking a clear gradual trend [79, 80]. The K–Pg extinction shows gradual signs of ocean acidification and volcanism, while the Chicxulub impact may have occurred 30,000 to 300,000 years before the main extinction event [7–9]. Physiological studies suggest that, under current gravity and atmospheric pressure, a fully erect neck posture in sauropods would have been physiologically improbable [81–85].

It is speculated that an MGC-PC event caused the extinction of the dinosaurs by destabilizing the crust, exposing the mantle, and releasing large volumes of volatiles into the atmosphere, leading to severe environmental instability. At that time, Earth may have had ~40–50% of its current mass, where dinosaurs could have evolved. Survival during this event would have favored aquatic organisms or those sheltered in isolated niches, including on the larger colliding planet.

### 4.7. Paleontology and Evolution of Life: Varve-type sedimentary rocks, tidal rhythmites, and shell fossils

Sedimentary rocks reflect the interaction between tides, glacial melting, and seasonal duration, providing insights into climatic cycles, gravitational variations, and orbital dynamics of each geological period.

Varves are laminated rocks formed in seasonal or glacial lakes, recording climatic and astronomical patterns such as solar and precession cycles. Examples occur in the Paleoproterozoic (~2.3 Ga), during the "Snowball Earth" (~720–635 Ma), between ~550–500 Ma, during intervals between extinctions (~420–360 Ma), and in the Permian (~320–280 Ma).

Evidence shows that Earth's rotation and orbital parameters have varied throughout geological time. Tidal rhythmites, dated between ~2450 and 620 Ma, and fossil shells dated to ~380 Ma and the Late Cretaceous (~84 Ma), indicate that a year once had between 435

and 369 days [86–91]. Speculatively, the MGC-PC cycle provides a theoretical framework that could explain abrupt changes, beyond the gradual effects attributed to lunar recession.

### 4.8. Astronomy and Planetary Sciences: Cycles of Geodynamic, Orbital, and Climatic Transformations in Earth's Evolution

This section synthesizes Earth's internal and orbital evolution according to the MGC-PC model, distributed across eight planetary fusion cycles over the past two billion years. Figure 4 – Planetary Coupling Cycle Diagram (MGC-PC): (a) sequence of fusion events, (b) simulated numerical parameters, and (c) main geological events temporally associated. Evidence for event (1) has been discussed in the previous sections, while that for the remaining events is detailed in references [92–108]. The proposed synchronization between MGC-PC events and paleontological/geological milestones is preliminary and has yet to undergo statistical testing and higher-resolution geochronological validation.

At each stage, the number of bodies is halved, ultimately forming a single planet with a mass equivalent to present-day Earth. Each event is linked to major geodynamic transformations, orbital variations, climate changes, and documented paleontological milestones. Some of these transformations may have coincided with significant changes in biodiversity, but this correlation remains preliminary and lacks statistical and geochronological validation. The proposed sequence integrates geological, fossil, and tidal records with theoretical simulations of progressive growth through successive fusions, providing a comprehensive view of the processes that shaped Earth's current configuration.

Sedimentary and fossil records indicate that the number of days in a year varied throughout geological time [86–91]. These data, combined with the identification of Milankovitch cycles in the Proterozoic record [109], suggest different orbital and rotational parameters. Within this context of Earth's evolutionary cycle, the gravitational capture of the Moon may have occurred only between ~750 and 66 Ma, with its orbit gradually circularized through interactions with nearby protoplanets. During this period, Earth would have had a mass greater than that of the Moon but only half of its current mass; therefore, gravitational interactions would have operated at a different intensity.

Studies indicate that gravitational interactions, orbital migration, and successive collisions were crucial for planetary evolution, favoring the capture of satellites and the ejection of small bodies into comet-like orbits [10–14, 110–116]. Grinin [113] interprets these processes as part of a broad evolutionary trajectory with multiple possible pathways, including stabilization, collisions, and capture. Blanc et al. [114] identify four main

mechanisms for the origin of satellites, among which the capture of heliocentric bodies is prominent. Repeated passages of massive bodies generate cumulative gravitational disturbances, eventually leading to collisions or ejections of smaller objects [115, 116].

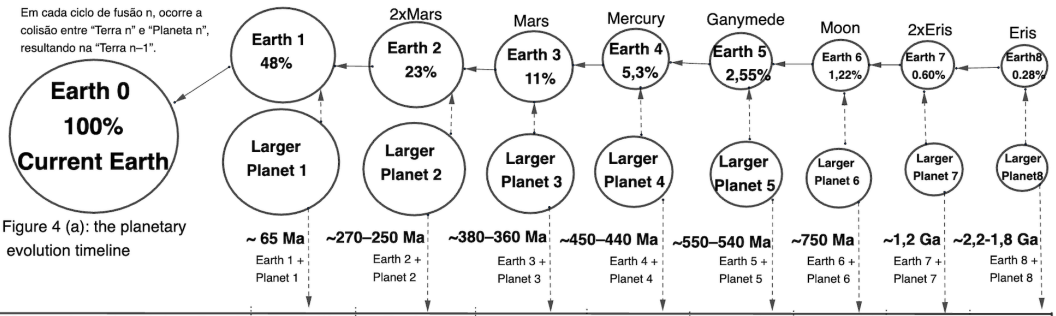


Figure 4 (a): the planetary evolution timeline

| Mass ratio 48% x 52% => Result: | Earth (0) | Earth (1) | Earth (2) | Earth (3) | Earth (4) | Earth (5) | Earth (6) | Earth (7) |
|---|---|---|---|---|---|---|---|---|
| Mass smaller planet (i) x current Earth | 48.00% | 23% | 11% | 5.3% | 2.55% | 1.22% | 0.60% | 0.28% |
| Densidade Earth (i) | 5,20E+03 | 4,88E+03 | 4,53E+03 | 4,18E+03 | 3,93E+03 | 3,43E+03 | 3,33E+03 | 3.09E+03 |
| Mass smaller planet (i) | 2.87E+24 | 1.38E+24 | 6.61E+23 | 3.17E+23 | 1.52E+23 | 7.30E+22 | 3.51E+22 | 1.68E+22 |
| Mass larger planet (i) | 3.11E+24 | 1.49E+24 | 7.16E+23 | 3.43E+23 | 1.65E+23 | 7.91E+22 | 3.80E+22 | 1.82E+22 |
| Resultant mass: Earth (i) | 5.97E+24 | 2.87E+24 | 1.38E+24 | 6.60E+23 | 3.17E+23 | 1,52E+23 | 7.30E+22 | 3.51E+22 |
| Resultant volume: Earth (i) (km) | 1.08E+12 | 5.51E+20 | 2.82E+20 | 1.46E+20 | 7.58E+19 | 3,87E+19 | 2.13E+19 | 1.05E+19 |
| Resultant surface: Earth (i) (km²) | 5.10E+08 | 3.25E+08 | 2.08E+08 | 1.34E+08 | 8.67E+07 | 5.53E+07 | 3.72E+07 | 2.33E+07 |
| Maximum ancient cratons: Earth (0) | 32% | 20% | 13% | 8,5% | 5,4% | 3,6% | 2,5% | 1,5% |
| Resultant radius: Earth (i) | 6,371 | 5,087 | 4,068 | 3,265 | 2,626 | 2,098 | 1,720 | 1,360 |
| Radius of smaller planet | 5,087 | 4,068 | 3,265 | 2,626 | 2,098 | 1,720 | 1,360 | 1,092 |
| Radius of larger planet | 5,224 | 4,178 | 3,353 | 2,697 | 2,155 | 1,766 | 1,397 | 1,121 |
| Gravitational force Earth (i) | 9.82 | 7.39 | 5,55 | 4.14 | 3.07 | 2.31 | 1.65 | 1.26 |
| Escape velocity smaller planet-km/s | 8.67 | 6.72 | 5.20 | 4.01 | 3.11 | 2.38 | 1.85 | 1.43 |
| Escape velocity larger planet-km/s | 8.91 | 6.90 | 5.34 | 4.12 | 3.20 | 2.45 | 1.90 | 1.47 |
| Escape velocity Earth (i)-km/s | 8.79 | 6.81 | 5.27 | 4.07 | 3.15 | 2.41 | 1.88 | 1.45 |
| System Impact Velocity-km/s, n=1 | 8.79 | 6.81 | 5.27 | 4.07 | 3.15 | 2.41 | 1.88 | 1.45 |
| System Impact Velocity-km/s, n=0,8 | 7.86 | 6.09 | 4.71 | 3.64 | 2.82 | 2.16 | 1.68 | 1.30 |
| Radius Hill smaller planet-km | 1,170,885 | 916,772 | 717,825 | 562,025 | 440,050 | 344,548 | 269,772 | 211,224 |
| Radius Hill larger planet-km | 1,202,545 | 941,561 | 737,201 | 577,222 | 451,949 | 353,864 | 277,066 | 216,936 |

Figure 4 (b): the numerical data

| Event (1) – ~66 Ma<br>Fusion: Earth 1 + Planet 1 = Current Earth | Event (2) – ~270–250 Ma<br>Earth 2+Planet 2=Earth 1 (mass≈2xMars) | Event (3) – ~380–360 Ma<br>Fusion: Earth 3 + Planet 3 = Earth 2 (mass≈Mars) |
|---|---|---|
| Detailed in Sections 4.1 to 4.7<br>.Core and Magnetic Anomalies<br>.Mantle heterogeneity<br>.Orogenic Processes, crustal Restructuring and Geodynamic Implications<br>.Petroleum and Mineral Reserves<br>.Biological Evolution, Extinctions<br>.Varve-type sedimentary rocks, tidal rhythmites, and shell fossils | .Permian extinction ~252 Ma.<br>Uralian orogeny subduction final around 250 Ma [92, 93]<br>.Oblique collision between Laurentia and Gondwana ~320–270 Ma result Alleghanian orogeny [94]<br>.Opening of the Meso-Tethys Ocean ~280 Ma and Neo-Tethys Ocean ~230 Ma [95]<br>.Subducction of the Paleo-Pacific plate ~260-250MA [96]<br>Triassic–Jurassic extinction (~201 Ma)<br>.Fossils ~84 Ma, 370 days per year [91]<br>.Florestas subtropicais e incêndios naturais no Norte da África ~84 Ma [97] | .Devonian extinction ~372-359 Ma[77]<br>.Orogenia uraliana (~380 Ma) subducção oceano Paleo-Uralian, colisão bloco cazaque e o cráton siberiano (~320–280 Ma) [92, 93]<br>.Opening of the Paleo-Tethys Ocean ~380 Ma [95]<br>.Diversification of vascular plants with deep root systems ~375–359 Ma [98, 99]<br>.Sedimentary records with organic deposition and the expansion of the first large trees around ~359 Ma [100]<br>.Decline in aquatic vertebrates and abruptclimate changes [101] |
| **Event (4) – ~450–440 Ma**<br>Earth 4+Planet 4=Earth 3 (mass≈Mercury) | **Event (5) – ~550–540 Ma**<br>Earth 5+Planet 5=Earth 4 (mass≈Ganymede) | **Event (6) – ~750 Ma**<br>Earth 6+Planet 6=Earth 5 (mass≈Moon) |
| .Ordovician–Silurian extinction ~443 Ma<br>.Closure of the Iapetus Ocean ~430–420 Ma<br>.Caledonian orogeny [102–103]<br>.Inner core radius ~40% of present Earth close to ~50% estimated by Zhou et al. [37] | .Cambrian Explosion ~541 Ma [78].<br>Very weak geomagnetic field ~550 Ma and aregenerated ~550 Ma [37]<br>.Fragmentation of the supercontinent Pannotia ~625–550 Ma [58]<br>.Formation of the Iapetus Ocean ~600–500 Ma [102] | .Breakup of Rodinia ~750 Ma [60, 63]<br>."Snowball Earth" glaciations ~717–635 Ma and ~584–579 Ma<br>.Low geodynamic activity, atmospheric changes, variations in insolation [105]<br>.Tidal records around ~620 Ma indicate a solar year of ~400 ± 7 days [87, 88] |
| **Event (7) – ~1.2 Ga**<br>Earth 7+Planet 7=Earth 6 (mass≈2xEris) | **Event (8) – ~2.2–1.8 Ga**<br>Earth 8+Planet 8=Earth 7 (mass≈Eris) | |
| .Dissolution of the Columbia supercontinent ~1.2 Ga, lithospheric–mantle reorganization and ~90° rotation of the North China Craton [106,107] | .Fragmentation of the Kenorland supercontinent ~2450–1850 Ma, formation of Huronian Basin (early stage) and Animikie Basin (late stage) [108]<br>.Asymmetric thermal subsidence within detachment fault systems<br>tidal rhythm records ~2450–1650 Ma indicate 384–435 days per year [86,87] | |

Figure 4 (c): the geological events

Figure 4 – Planetary Coupling Cycle Diagram (MGC-PC)

An MGC-PC cycle introduces new parameters that complement the analysis of satellite capture, comet ejection, and the fragmentation of bodies in the asteroid belt region. These parameters involve the presence of multiple protoplanets in nearby orbits and the lower mass of planets in earlier stages. Thus, satellites could have been captured, and comets ejected, during these less energetic phases in the evolution of these celestial bodies. This allows speculation that Earth, in the past, may have hosted additional satellites that were later destabilized by the approach of another massive planet. As an illustration, a near free-fall impact of a satellite the size of Deimos could have produced structures comparable to the largest known craters, such as Chicxulub.

Chambers [1] suggests that "something went wrong" in the asteroid belt region, whereas the MGC-PC model allows speculation that planetary evolution there was almost successful, culminating in the formation of two protoplanets. A collision at the intersection of their orbits, at a typical orbital velocity for the region, would have resulted in an impact of 18 km/s—nearly twenty times greater than the local escape velocity, which would not have exceeded 1 km/s. Under such conditions, the collision would have fragmented the two hypothetical protoplanets, giving rise to the asteroid belt.

***Water cycle in Earth's evolutionary cycle:*** The MGC-PC cycle (Figure 4) allows speculation on water dynamics and the interpretation of evidence related to deep heterogeneities and hydrothermal flows. In this context, it is possible that large volumes of oceanic water were buried during fusion events, interacting within interface zones between the merged bodies. However, smaller planets would have had reduced surface areas and a lower capacity to incorporate water into the mantle during fusion. In these earlier stages, the protoplanets may have contained either less or more liquid water, depending on their origins. In this context, it is speculated that, throughout the proposed stages in the evolution of the bodies that formed present-day Earth, many of these worlds may have been entirely covered by oceans.

Currently, the presence of water in Earth's interior is observed in the transition zone, with estimated volumes equivalent to up to three oceans [38–41], while variations in average sea level over the past 540 million years [117] may reflect a dynamic relationship between surface water volume and planetary surface area at each stage. On the other hand, Barrett et al. [118], based on analyses of enstatite chondrite (EC) meteorites—considered analogs of Earth's building blocks—suggest that hydrogen and water were already present in significant amounts within the planet since the original formation of these materials. Rohling et al. [119]

indicate that deep-ocean temperatures remained high between ~60 and 40 Ma, followed by a progressive cooling throughout the Cenozoic. A proposed MGC-PC event around ~66 Ma could have heated ocean waters through direct contact with exposed mantle.

### 4.9. Astronomy and Planetary Sciences: Evidence of MGC-PC on Venus, Mars, and Mercury

The MGC-PC model speculatively suggests a reinterpretation of structural and orbital features on Venus, Mars, and Mercury as possible remnants of planetary mergers, similar to what is proposed for Earth.

***Venus:*** The planet may have had a habitable climate until around 700 Ma [120], with its crust possibly resurfaced between 700 and 300 Ma [121, 122]. Recent models attribute its retrograde rotation to atmospheric tides and core-mantle friction, rather than giant impacts [123]. Venus lacks active plate tectonics and displays features such as Maxwell Montes (analogous to orogenic belts), southern hemisphere plains, and depressions between Ishtar Terra and Aphrodite Terra. Dias et al. [124] simulate volcanic plumes containing water vapor in Venus's night atmosphere, associated with the release of interior volatiles.

***Mars:*** The Martian surface features the Boreal Basin, with an asymmetric and hemispheric-scale shape, possibly representing an impact depression bordered by Tharsis and Arabia Terra, structures resembling continental blocks. Additionally, it is marked by hemispheric dichotomy, crustal variations, and magnetic contrasts. Valantinas et al. [125] confirm the presence of ferrihydrite, formed in cold and wet environments, and point to indirect evidence of episodic, dynamic, and global events in Mars' past.

***Mercury:*** The planet exhibits high density and low mass, along with a basin and a plain that may represent ancient seas.

### 4.10. Model Limitations and Potential Contributions of the MGC-PC Hypothesis

The literature highlights open questions regarding the evolutionary pathways of the planets in the Solar System. These gaps include physicochemical, orbital, and impact modeling aspects, revealing limitations in the integration of gravitational processes, geochemical effects, and non-catastrophic fusion scenarios [10–14, 19, 25, 26, 110–112]. In this context, although speculative in some respects, the MGC-PC hypothesis emerges as a unifying approach to planetary collisions and mergers, consistent with observed physical and isotopic evidence.

| Aspect | Conventional Models | MGC-PC Hypothesis |
|---|---|---|
| Fusion of differentiated bodies | Partial or destructive collisions not predicted | Core mechanism of complete fusion of planetary bodies |
| Internal structural recomposition | Absent or rarely considered | Explains coalescence and reassembly of planetary layers |
| Internal heterogeneities | Attributed to chemical evolution | Explains mantle heterogeneities, ULVZs, water, and organic matter |
| Magnetic field | Linked to core cooling | Fusion/reorganization of cores, multiple dipoles |
| Mass extinctions | Consequences without clearly defined cause | Defines causes, including gravitational influence |
| Crustal profile | Isolated process analysis | Integrated analysis of crustal morphology |
| Mineral deposits | Volcanism and water transport | Unique transport of soluble and insoluble elements |
| Petroleum origin | Biogenic or abiogenic | Organic matter from extinctions, trapped in mantle and oceans |
| Satellites and comets | Impacts or co-accretion | Gravitational capture and ejection |
| Interdisciplinary integration | Limited to specific domains | Integrates geodynamics, paleontology, astrobiology |
| Deep geochemical anomalies | Rare plume leaks | Homogeneous core-mantle mixing during fusion |
| Fossils and sedimentary rocks | Small orbital variations within stable orbits | Sedimentary cycles and climatic changes post-fusion. |

Table 1. Comparison between Conventional Models and the MGC-PC Hypothesis

***Limitations of the MGC-PC model:*** The morphological signatures predicted for a fusion process of differentiated planetary bodies, as well as their correlation with observable evidence in the inner planets, do not directly depend on the simplifications adopted in this study. The limitations are mainly related to the assessment of impact velocity and the critical conditions required for planetary fusion.

The analysis does not include material loss, chemical composition, mantle viscosity, or detailed thermal effects. Gravity and energy dissipation are considered, with a 20% rate based on previous studies. This value may vary with composition, ocean presence, and impact angle. Lower rates hinder fusion but do not affect the condition of sub-critical impact velocity. Residual orbital differences were not evaluated.

The results were obtained using simple analytical models, calculated in Excel based on Newton's and Kepler's laws. Gravity, velocities, and radii were derived from mass, density, the gravitational constant (G), and average solar distance. Gravitational attraction assumed the bodies were initially at rest relative to each other, without N-body simulations, SPH methods, or advanced computational codes. The goal was to establish a preliminary physical framework compatible with future simulations using tools such as REBOUND, GADGET-2, or pkdgrav.

## 5. Conclusion

This proposal complements current models by analyzing non-destructive collisions of planetary bodies predicted by astronomy and proposing the mass fusion process, highlighting its long-lasting morphological signatures. Furthermore, it correlates these signatures with widely studied observable evidence, which is currently treated in isolation across different existing models.

The hypothesis introduces an innovative perspective on the growth of rocky planets, suggesting that they doubled their mass through successive planetary coupling events (MGC-PC), resulting in the formation of a new planetary body. In these fusion events, the mantle of the smaller body spreads over the larger one, partially preserving its crust and forming new geological structures. The resulting signatures include mantle heterogeneities, inner core growth, magnetic anomalies, internal boundary zones, orbital variations, mass extinctions, and orogeny. The hypothesis also suggests a solid multi-spherical inner core immersed in a liquid medium, including water, as a possible explanation for observed anomalies in Earth's core.

Earth may have undergone eight MGC-PC events, the most recent occurring around 66 Ma, with an estimated impact velocity of 7.86 km/s, below the escape velocity of 8.79 km/s. Under these conditions, a non-destructive fusion with partial preservation is supported by multidisciplinary evidence. Its validation can be confirmed through comprehensive simulations and supported by future research focusing on the following key areas:

- Numerical simulations of mutual gravitational capture within the Hill sphere, analyzing the influence of varying masses, angles, and orbital velocity differences between bodies on impact velocity;
- Seismic modeling of the inner core to detect multiple solid spheres, variations in their shape and composition, and magnetic anomalies associated with the agglomeration of iron, liquid iron-nickel, and water under high pressure;
- Geochemical analyses of hotspots, Yellowstone, SAMA, and mantle plumes for potential heterogeneities involving mantle material and outer core mixing;
- High-pressure interactions among water, volatiles, organic matter, and buried crust within the interface zone as potential sources of hydrocarbons and hydrogen;
- Integrated reinterpretation of tectonic cycles, orogenic processes, mineral deposition, and mass extinctions in light of MGC-PC events and their orbital effects;.

In summary, the MGC hypothesis proposes a conceptual reorganization based on testable evidence, opening new perspectives for understanding planetary evolution and requiring future validation through mathematical models and comparison with geological and orbital records.

The limitations of current models are widely recognized in studies of orbital evolution and planetary mass dynamics, and each of them may, in its own way, incorporate the new parameters offered by the MGC-PC model. The methodological limitations of the present study, such as the absence of high-complexity numerical simulations and the simplification of physical parameters, however, do not compromise the proposed analysis of the planetary fusion process nor the correlation of its morphological signatures with the broad range of geophysical, geochemical, and astronomical evidence already studied by science. Thus, these methodological constraints do not undermine the physical consistency of the MGC-PC hypothesis, which remains valid and potentially useful for improving existing models while awaiting its full validation.

**Acknowledgments**
This article is dedicated, with deep respect, to the late Dimas Candido Waltrick, whose conviction that the Pacific Ocean represents an impact crater inspired the beginning of this journey.
The author thanks Charlesworth Author Services for editorial assistance and the anonymous reviewers, whose comments were fundamentally important to this version.
I extend my gratitude to the researchers who made their findings publicly available, whom I consider true mentors from a distance, as well as to those with whom I had the opportunity to clarify specific questions.

**Data Availability**
All relevant data are available within the article.

**Competing Interests**
The author declares no competing interests.

**Funding**
No external funding was received for this work.

**Author's Note**
This article is a contribution to the advancement of open, multidisciplinary science grounded in observable reality. It was developed with the support of ChatGPT as a tool for organizing and refining language, an invisible ally throughout the process, without interfering with authorship or the formulation of hypotheses. After all, knowledge not shared is knowledge lost.

## References

1. Neumann V, Ma N, Bouvier A, Trieloff M. 2024 Formação planetesimal recorrente em uma parte externa do início do sistema solar. Scientific Reports 14, 1417, https://doi.org/10.1038/s41598-024-63768-4

2. Chambers JE. 2004 Planetary accretion in the inner Solar System. Earth Planet. Sci. Lett. 223, 241-252 https://doi.org/10.1016/j.epsl.2004.04.031

3. Canup RM. 2004 Simulations of a late lunar-forming impact. Icarus 168, 433–456, https://doi.org/10.1016/j.icarus.2003.09.028

4. Cuk M, Stewart ST. 2012 Making the moon from a fast-spinning Earth: A giant impact followed by resonant despinning. Science 338, 1047–1052, https://doi.org/10.1126/science.1225542

5. Kendall JD, Melosh HJ. 2016 Differentiated planetesimal impacts into a terrestrial magma ocean: fate of the iron core. Earth Planet. Sci. Lett. 448, 24–33, https://doi.org//10.1016/j.epsl.2016.05.012

6. Morbidelli A, Tsiganis K, Batygin K, Crida A, Gomes R. 2012 Explaining why the uranian satellites have equatorial prograde orbits despite the large planetary obliquity. Icarus 219, 737–740, https://doi.org/10.1016/j.icarus.2012.03.025

7. Renne PR, Deino AL, Hilgen FJ, Kuiper KF, Mark DF, Mitchell III WS. et al. 2013 Time scales of critical events around the Cretaceous–Paleogene boundary. Science 339, 684–687, https://doi.org/10.1126/science.1230492

8. Keller G, Mateo P, Monkenbusch J, Thibault N, Punekar J, Spangenberg JE. Et al. 2020 Mercury linked to Deccan Traps volcanism, climate change and the end-Cretaceous mass extinction. Global and Planetary Change 194, 103312 https://doi.org/10.1016/j.gloplacha.2020.103312

9. Keller G. 2012 The Cretaceous–Tertiary mass extinction, Chicxulub impact, and Deccan volcanism. In: Talent JA (ed.) Earth and Life. International Year of Planet Earth. Springer (Livro), Dordrech 759-793 https://doi.org/10.1007/978-90-481-3428-1_25

10. Bizzarro M, Johansen A, Dorn C. 2025 The cosmochemistry of planetary systems. Nature Reviews Chemistry, 9, 378-396 https://doi.org/10.1038/s41570-025-00711-9

11. Crossley SD, Setera JB, Anzures BA, Iacovino K, Buckley WP, Eckley SA, et al. 2025 Percolative sulfide core formation in oxidized planetary bodies. Nature Communications, 16, 3233, https://doi.org/10.1038/s41467-025-58517-8

12. Ipatov SI. 2024 Migration of Celestial Bodies in the Solar System and in Some Exoplanetary Systems. Solar System Research, 58, S50-S63, https://doi.org/10.1134/S0038094623600105

13. Raymond SN, Izidoro A, Morbidelli A. 2020 Solar system formation in the context of extrasolar planets. Planetary Astrobiology, 287-307, https://doi.org/10.2458/azu_uapress_9780816540068

14. Raymond SN. 2024 The Solar System: structural overview, origins and evolution. arXiv preprint (arXiv:2404.14982), https://arxiv.org/abs/2404.14982.

15. Asphaug E. 2014 Impact origin of the Moon? Annual Review of Earth and Planetary Sciences. 42, 551–578 https://doi.org/10.1146/annurev-earth-050212-124057

`

16. Biggin AJ, Steinberger B, Aubert J, Suttie N, Holme R, Torsvik TH. et al. 2012 Possible links between long-term geomagnetic variations and convection processes of the entire mantle. Nature Geoscience 5, 526–533, https://doi.org/10.1038/ngeo1521

17. Dannberg J, Gassmoeller R, Thallner D, LaCombe F, Sprain C. 2023 Changes in core-mantle boundary heat flux patterns throughout the supercontinent cycle. Geophysical Journal International 237, 1251–1274, https://doi.org/10.1093/gji/ggae075

18. Genda H, & Abe Y. 2005 Enhanced atmospheric loss on protoplanets at the giant impact phase in the presence of oceans. Nature 433, 842–844, https://doi.org/10.1038/nature03360

19. Collins GS, Melosh j, Osinsk GR. 2012 The impact-cratering process. Elements 8, 25–30, https://doi.org/10.2113/gselements.8.1.25

20. Genda H, Kokubo E, Ida S. 2012 Merging criteria for giant impacts of protoplanets. The Astrophysical Journal 744, 137, https://doi.org/10.1088/0004-637X/744/2/137

21. Kegerreis J, Eke V, Catling D, Massey R, Teodoro L, Zahnle K. 2020 Atmospheric erosion by giant impacts onto terrestrial planets: A scaling law for any speed, angle, mass, and density. The Astrophysical Journal Letters 901, L31, https://doi.org/10.3847/2041-8213/abb5fb

22. Denman TR, Leinhardt ZM, Carter PJ. 2022 Atmosphere loss in oblique Super-Earth collisions. Monthly Notices of the Royal Astronomical Society 513, 1680–1700, https://doi.org/10.1093/mnras/stac923

23. Emsenhuber A, Asphaug E. 2019 Graze-and-merge collisions under external perturbers. The Astrophysical Journal 881, 102, https://doi.org/10.3847/1538-4357/ab2f8e

24. Emsenhuber A, Cambioni s, Asphaug E, Gabriel TSJ, Schwartz SR, Furfaro R. 2020 Realistic on-the-fly outcomes of planetary collisions. II. Bringing machine learning to N-body simulations. The Astrophysical Journal 891, 6, https://doi.org/10.3847/1538-4357/ab6de5

25. Asphaug E, Agnor CB, Williams Q. 2006 Hit-and-run planetary collisions. Nature 439, 155–160, https://doi.org/10.1038/nature04311

26. Canup RM, Asphaug E. 2001 Origin of the Moon in a giant impact near the end of the Earth's formation. Nature 412, 708-712, https://doi.org/10.1038/35089010

27. Jutzi M, Benz W. 2016 Formation of bi-lobed shapes by sub-catastrophic collisions: A late origin of comet 67P/C-G's structure. Astronomy & Astrophysics 597, A62, https://doi.org/10.1051/0004-6361/201628964

28. Hu S, Ji J, Richardson DC, Zhao Y, Zhang Y. 2018 The formation mechanism of 4179 Toutatis' elongated bilobed structure in a close Earth encounter scenario. Monthly Notices of the Royal Astronomical Society 478, 501–515, https://doi.org/10.1093/mnras/sty1073

29. Zhao Y, Ji J, Huang J, Hu S, Hou X, Li Y. et al. 2015 Orientation and rotational parameters of asteroid 4179 Toutatis: new insights from Chang'e-2's close flyby. Monthly Notices of the Royal Astronomical Society 450, 3620–3632, https://doi.org/10.1093/mnras/stv792

30. Savage PS, Moynier F, Chen H, Shofner G, Siebert J, Badro J, et al. 2015 Copper isotope evidence for large-scale sulphide fractionation during Earth's differentiation. Geochemical Perspectives Letters 1, 53–64, https://doi.org/10.7185/geochemlet.1506

31. Wang W, Vidale JE, Pang G, Koper KD, Wang R. 2024 Inner core backtracking by seismic waveform change reversals. Nature 631, 340–343, https://doi.org/10.1038/s41586-024-07536-4

32. Vidale JE, Wang W, Wang R, Pang G, Koper K. 2025 Annual scale variability in both rotation rate and near-surface of the Earth's inner core. Nature Geoscience 18, 267–272, https://doi.org/10.1038/s41561-025-01642-2

33. Vidale JE, Wang W, Wang R, Pang G, Koper KD. 2025 Earth's mysterious inner core really is changing shape. Nature 638, 593-594, https://doi.org/10.1038/d41586-025-00395-7

34. Mäkinen AM, Deuss A. 2011 Global seismic body-wave observations of temporal variations in the Earth′s inner core, and implications for its differential rotation. Geophysical Journal International 187, 355–370, https://doi.org/10.1111/j.1365-246X.2011.05146.x

35. He Y, Sun S, Kim DY, Jang BG, Li H, Mao HK. 2022 Superionic iron alloys and their seismic velocities in Earth's inner core. Nature 602, 258–262, https://doi.org/10.1038/s41586-021-04361-x

36. Deuss A. 2014 Heterogeneity and Anisotropy of Earth's Inner Core. Annual Review of Earth and Planetary Sciences, 42, 103-126. https://doi.org/10.1146/annurev-earth-060313-054658

37. Zhou T, Tarduno JA, Nimmo F, Cottrell RD, Bono RK, Ibanez-Mejia M. et al. 2022 Early Cambrian renewal of the geodynamo and the origin of inner core structure. Nature Communications 13, 4161, https://doi.org/10.1038/s41467-022-31677-7

38. Pearson DG, Brenker FE, Nestola F, McNeill J, Nasdala L, Hutchison MT. et al. 2014 Hydrous mantle transition zone indicated by ringwoodite included within diamond. Nature 507, 221–224, https://doi.org/10.1038/nature13080

39. Gu T, Pamato MG, Novella D, Alvaro M, Fournelle J, Brenker FE. et al. 2022 Hydrous peridotitic fragments of Earth's mantle 660 km discontinuity sampled by a diamond. Nature Geoscience 15, 950–954, https://doi.org/10.1038/s41561-022-01024-y

40. Huang X, Xu Y, Karato S. 2005 Water content in the transition zone from electrical conductivity of wadsleyite and ringwoodite. Nature 434, 746–749, https://doi.org/10.1038/nature03426

41. Hallis LJ, Huss GR, Nagashima K, Taylor GJ, Halldórsson SA, Hilton DR. et al. 2015 Evidence for primordial water in Earth's deep mantle. Science 350, 795–797, https://doi.org/10.1126/science.aac4834

42. Brenker FE, Vincze L, Vekemans B, Nasdala L, Stachel T, Vollmer C. et al. 2005 Detection of a Ca-rich lithology in the Earth's deep (> 300 km) convecting mantle. Earth Planet. Sci. Lett. 236, 579–587, https://doi.org/10.1016/j.epsl.2005.05.021

43. Finlay CC, Kloss C, Olsen N, Hammer MD, øffner-Clausen L, Grayver A. et al. 2020 The CHAOS-7 geomagnetic field model and observed changes in the South Atlantic Anomaly. Earth Planets and Space 72, 156, https://doi.org/10.1186/s40623-020-01252-9

44. Nordstrom DK, McCleskey RB, Ball JW. 2009 Sulfur geochemistry of hydrothermal waters in Yellowstone National Park: IV Acid–sulfate waters. Applied Geochemistry 24, 191–207, https://doi.org/10.1016/j.apgeochem.2008.11.019

45. Hansen SE, Garnero EJ, Li M, Shim SH, Rost S. 2023 Globally distributed subducted materials along the Earth's core-mantle boundary: Implications for ultralow velocity zones. Science Advances 9, eadd4838, https://doi.org/10.1126/sciadv.add4838

46. Qian Y, Li M, Desch SJ, Ko B, Deng H, Garnero EJ. et al. 2023 Moon-forming impactor as a source of Earth's basal mantle anomalies. Nature 623, 95–99, https://doi.org/10.1038/s41586-023-06589-1

47. Wang J, Lekić V, Schmerr NC, Gu YJ, Guo Y, Lin R. 2024 Mesozoic intraoceanic subduction shaped the lower mantle under the East Pacific uplift. Science Advances 10, eado1219, https://doi.org/10.1126/sciadv.ado1219

48. Feng J, Yao H, Wang Y, Poli P, Mao Z. 2021 Segregated oceanic crust trapped at the bottom mantle transition zone revealed from ambient noise interferometry. Nature Communications 12, 2531, https://doi.org/10.1038/s41467-021-22853-2

49. Torsvik TH, Steinberger B, Ashwal LD, Doubrovine PV, Tronnes RG. 2016 Evolution and dynamics of the Earth – a tribute to Kevin Burke. Canadian Journal of Earth Sciences 53, 1073-1087, https://doi.org/10.1139/cjes-2015-0228

50. Vaes B, van Hinsbergen DJJ. 2025 Slow True Polar Wander Around Varying Equatorial Axes Since 320 Ma. AGU Advances 6, e2024AV001515, https://doi.org/10.1029/2024AV001515

51. van Hinsbergen DJJ, Steinberger B, Guilmette C, Maffione M, Gürer D, Peters K. et al. 2021 A record of plume-induced plate rotation triggering subduction initiation. Nature Geoscience 14, 626–630, https://doi.org/10.1038/s41561-021-00780-7

52. Messling N, Willbold M, Kallas L, Elliott T, Fitton JG, Müller T, et al. 2025 Ru and W isotope systematics in ocean island basalts reveals core leakage. Nature 642, 376-380, https://doi.org/10.1038/s41586-025-09003-0

`

53. Rojas-Agramonte Y, Pardo N, van Hinsbergen DJJ, Winter C, Marroquín-Gómez MP, Liu S, et al. 2024 Zircon xenocrysts from Easter Island (Rapa Nui) reveal hotspot activity since the middle Jurassic. AGU Advances 5, e2024AV001351, https://doi.org//10.1029/2024AV001351

54. Rojas-Agramonte Y, Kaus BJ, Piccolo A, Williams IS, Gerdes A, Wong J. et al. 2022 Zircon dates long-lived plume dynamics in oceanic islands. Geochemistry, Geophysics, Geosystems 23, e2022GC010485, https://doi.org/10.1029/2022GC010485

55. Greenough JD, Kamo SL, Davis DW, Larson K, Zhang Z, Layton-Matthews D. et al. 2021 Old subcontinental mantle zircon below Oahu. Communications Earth & Environment 2, 189, https://doi.org/10.1038/s43247-021-00261-0

56. Kupenko I, Aprilis G, Vasiukov DM, McCammon C, Chariton S, Cerantola V. et al. 2019 Magnetism in cold subducting slabs at mantle transition zone depths. Nature 570, 102–106, https://doi.org/10.1038/s41586-019-1254-8

57. Valdiya KS. 1984 Evolution of the Himalaya. Tectonophysics 105, 229–248, https://doi.org/10.1016/0040-1951(84)90205-1

58. Rowley DB. 1996 Age of initiation of collision between India and Asia: A review of stratigraphic data. Earth Planet. Sci. Lett. 145, 1–13, https://doi.org/10.1016/S0012-821X(96)00201-4

59. Hoke GD, Garzione CN. 2008 Paleosurfaces, paleoelevation, and the mechanisms for the late Miocene topographic development of the Altiplano plateau. Earth Planet. Sci. Lett. 271, 192–201, https://doi.org/10.1016/j.epsl.2008.04.008

60. Nance RD, Brendan Murphy JB. 2019 Supercontinents and the case of Pannotia. Geological Society, London, Special Publications 470, 65-86, https://doi.org/10.1144/SP470.5

61. Nance RD, Murphy B, Santosh M. 2014 The supercontinent cycle: A retrospective essay. Gondwana Research 25, 4–29, https://doi.org/10.1016/j.gr.2012.12.026

62. Pastor-Galán D, Nance RD, Murphy JB, Spencer CJ. 2019 Supercontinents: myths, mysteries, and milestones. Geological Society, London, Special Publications 470, 39–64, https://doi.org/10.1144/SP470.16

63. Bond GC, Nickeson PA, Kominz MA. 1984 Breakup of a supercontinent between 625 Ma and 555 Ma: new evidence and implications for continental histories. Earth Planet. Sci. Lett. 70, 325-345, https://doi.org/10.1016/0012-821X(84)90017-7

64. van Hinsbergen DJJ, Torsvik TH, Schmid SM, Maţenco LC, Maffione M, Vissers RLM, Et al. 2019 Orogenic architecture of the Mediterranean region and kinematic reconstruction of its tectonic evolution since the Triassic. Gondwana Research 81, 79–229, https://doi.org/10.1016/j.gr.2019.07.009

65. Kutcherov VG, Krayushkin VA. 2010 Deep-seated abiogenic origin of petroleum: From geological assessment to physical theory. Reviews of Geophysics 48, RG1001, https://doi.org/10.1029/2008RG000270

66. Höök M, Bardi U, Feng L, Pang X. 2010 Development of oil formation theories and their importance for peak oil. Marine and Petroleum Geology 27, 1995-2004, https://doi.org/10.1016/j.marpetgeo.2010.06.005

67. Sleep NH, Bird DK, Pope E. 2012 Paleontology of the Earth's Mantle. Paleontology of Earth's mantle. Annu. Rev. Earth Planet. Sci. 40, 277-300, https://doi.org/10.1146/annurev-earth-092611-090602

68. Hein FJ, Cotterill DK. 2006 The Athabasca Oil Sands – A regional geological perspective, Fort McMurray area, Alberta, Canada. Natural Resources Research 15, 85–102, https://doi.org/10.1007/s11053-006-9015-4

69. Li Y, Zhang X, Xin S, Liu W. 2019 Evolution of Persian Gulf Basin and formation of super-large oil and gas fields. Geology in China, https://doi.org/10.11781/sysydz201904548

70. Fischer-Gödde M, Tusch J, Goderis S, Bragagni A, Mohr-Westheide T, Messling N. et al. 2024 Ruthenium isotopes show the Chicxulub impactor was a carbonaceous-type asteroid. Science 385, 752–756, https://doi.org/10.1126/science.adk4868

71. Fouquet Y, Auclair G, Cambon P, Etoubleau J. 1988 Geological setting and mineralogical and geochemical investigations on sulfide deposits near 13°N on the East Pacific Rise. Marine Geology 84, 145-178, https://doi.org/10.1016/0025-3227(88)90098-9

72. Javoy M, Kaminski E. 2014 Earth's Uranium and Thorium content and geoneutrinos fluxes based on enstatite chondrites. Earth Planet. Sci. Lett. 407, 1-8, https://doi.org/10.1016/j.epsl.2014.09.028

73. Berezhnaya ED, Dubinin AV. 2017 Determination of the platinum-group elements and gold in ferromanganese nodule reference material NOD-A-1. Geochemistry International, 55, 218-224, https://doi.org/10.1134/S0016702917010037

74. Brusatte SL, Mordomo RJ, Barrett PM, Carrano MT, Evans DC, Lloyd GT, et al. 2015 The extinction of the dinosaurs. Biological Reviews 90, 628–642, https://doi.org/10.1111/brv.12128

75. Barrera E, Savin, SM. 1999 Evolution of late Campanian-Maastrichtian marine climates and oceans. In Evolution of the Cretaceous Ocean-Climate System. Geological Society of America; Special Paper 332, 245–282, https://doi.org/10.1130/0-8137-2332-9.245

76. Courtillot VE, Renne PR. 2003 On the ages of flood basalt events. Comptes Rendus Geoscience 335, 113–140, https://doi.org/10.1016/S1631-0713(03)00006-3

77. Montañez, IP. 2022 Current synthesis of the penultimate icehouse and its imprint on the Upper Devonian through Permian stratigraphic record. Geological Society, London, Special Publications, 512, 213–245, https://doi.org/10.1144/SP512-2021-124

`

78. Zhang XL, Shu DG. 2013 Causes and consequences of the Cambrian explosion. Science China Earth Sciences, 57, 930–942, https://doi.org/10.1007/s11430-013-4751-x

79. Long JA, Niedźwiedzki G, Garvey J, Clement AM, Camens AB, Eury CA, et al. 2025 Earliest amniote tracks recalibrate the timeline of tetrapod evolution. Nature, 641,1193–1200, https://doi.org/10.1038/s41586-025-08884-5

80. Dean CD, Chiarenza AA, Doser JW, Farnsworth A, Jone LA, Et al. 2025 The structure of the end-Cretaceous dinosaur fossil record in North America. Current Biologu 35, p1973-1968.E6, https://doi.org/10.1016/j.cub.2025.03.025

81. Seymour RS, Lillywhite HB. 2000 Hearts, neck posture and metabolic intensity of sauropod dinosaurs. Proceedings of the Royal Society of London. Series B: Biological Sciences 267, 1883–1887, https://doi.org/10.1098/rspb.2000.1225

82. Snelling EP, Seymour RS. 2024 The hearts of large mammals generate higher pressures, are less efficient and use more energy than those of small mammals. Journal of Experimental Biology, 227, jeb247747, https://doi.org/10.1242/jeb.247747

83. Seymour RS, Lillywhite HB. 2016 Why vascular siphons with sub-atmospheric pressures are physiologically impossible in sauropod dinosaurs. Journal of Experimental Biology, 219, 2078–2080, https://doi.org/10.1242/jeb.137505

84. Seymour RS. 2016 Cardiovascular Physiology of Dinosaurs. American Physiological Society, https://doi.org/10.1152/physiol.00016.2016

85. Seymour RS. 2009 Raising the sauropod neck: it costs more to get less. Biology Letters, 5, 317–319, https://doi.org/10.1098/rsbl.2009.0096

86. Williams GE. 2000 Geological Constraints on the Precambrian History of Earth's Rotation and the Moon's Orbit. Reviews of Geophysics 38, 37-59, https://doi.org/10.1029/1999RG900016

87. Mazumder R. 2004 Implications of lunar orbital periodicity from the Chaibasa tidal rhythmite (India) of late Paleoproterozoic age. Geology 32, 841–844, https://doi.org/10.1130/G20424.1

88. Williams GE. 1998 Precambrian tidal and glacial clastic deposits: Implications for Precambrian Earth-Moon dynamics and palaeoclimate. Sedimentary Geology 120, 55–74, https://doi.org/10.1016/S0037-0738(98)00027-X

89. Wells JW. 1963 Coral growth and geochronometry. Nature 197, 948–950, https://doi.org/10.1038/197948a0

90. Scrutton, CT. 1978 Periodic growth features in fossil organisms and the length of the day and month. Tidal Friction and the Earth's Rotation (Book, Springer) 154–196, https://doi.org/10.1007/978-3-642-67097-8_12)

`

91. de Winter NJ, Goderis S, van Malderen SJM, Sinnesael M, Vansteenberge S, Snoeck C, et al. 2020 Subdaily-scale chemical variability in a Torreites sanchezi rudist shell: Implications for rudist paleobiology and the Cretaceous day–night cycle. Paleoceanography Paleoclimatology, 35, e2019PA003723, https://doi.org/10.1029/2019PA003723

92. Puchkov VN. 2009 The Evolution of the Uralian Orogen. Geological Society, London, Special Publications 327, 161–195, https://doi.org/10.1144/SP327.9

93. Puchkov VN. 1997 Structure and Geodynamics of the Uralian Orogen. In: Burg, J.P. & Ford, M. (eds) Orogeny Through Time. Geological Society, London, Special Publications 121, 201–236, https://doi.org/10.1144/GSL.SP.1997.121.01.09

94. Hopper E, Fischer KM, Wagner LS, Hawman RB. 2017 Reconstructing the end of the Appalachian orogeny. Geology 45, 15–18, https://doi.org/10.1130/G38453.1

95. Metcalfe I. 2013 Gondwana dispersion and Asian accretion: Tectonic and palaeogeographic evolution of eastern Tethys. Journal of Asian Earth Sciences 66, 1-33, https://doi.org/10.1016/j.jseaes.2012.12.020

96. Allen MB, Song S, Wang C. 2025 An invasion model for the start of Paleo-Pacific subduction. Geology 53, 488–492, https://doi.org/10.1130/G53022.1

97. Atfy HE, Sallam H, Jasper A, Uhl D. 2016 The first evidence of paleo-wildfire from the Campanian (Late Cretaceous) of North Africa. Cretaceous Research 57, 306–310, https://doi.org/10.1016/j.cretres.2015.09.012

98. Kenrick P, Crane PR. 1997 The origin and early evolution of plants on land. Nature 389, 33-39, https://www.nature.com/articles/37918

99. Morris JL, Puttick MN, Clark JW, Edwards D, Kenrick P, Pressel S. et al. 2018 The timescale of early land plant evolution. Proceedings of the National Academy of Sciences of the USA (PNAS), 115, E2274-E2283, https://doi.org/10.1073/pnas.1719588115

100. Wohl E. 2013 Floodplains and wood. Earth-Sci. Rev. 123, 194–212, https://doi.org/10.1016/j.earscirev.2013.04.009

101. Kaiser SI, Aretz M, Becker RT. 2016 The global Hangenberg Crisis (Devonian–Carboniferous transition): review of a first-order mass extinction. Geological Society, London, Special Publications 423, 387-437, https://doi.org/10.1144/SP423.9

102. Corfu F, Gasser D, Chew DM. 2014 New perspectives on the Caledonides of Scandinavia and related areas: introduction. Geological Society 390, 1–8, https://doi.org/10.1144/SP390.28

103. Corfu F, Andersen TB, Gasser D. 2015 The Scandinavian Caledonides: main features, conceptual advances and critical questions. Geological Society London 390, 9-43, https://doi.org/10.1144/SP390.25

104. Gee DG, Henriksen N. 2008 From the Early Paleozoic Platforms of Baltica and Laurentia to the Caledonide Orogen of Scandinavia and Greenland. Episodes 31, 44-51, https://doi.org/10.18814/epiiugs/2008/v31i1/007

105. Casado JA. 2021 A Review of Neoproterozoic Global Glaciations and a Biotic Cause of Them. Earth Systems and Environment, 5, 811–824, https://doi.org/10.1007/s41748-021-00258-x

106. Liu B, Jin S, Tian G, Li L, Qin Y, Xie Z, et al. 2024 Mesoproterozoic (ca. 1.3 Ga) A-Type Granites on the Northern Margin of the North China Craton: Response to Break-Up of the Columbia Supercontinent. Minerals 14, 622, https://doi.org/10.3390/min14060622

107. Roberts NMW. 2013 The boring billion? – Lid tectonics, continental growth and environmental change associated with the Columbia supercontinent. Geoscience Frontiers 4, 681-691, https://doi.org/10.1016/j.gsf.2013.05.004

108. Young GM. 2015 Did prolonged two-stage fragmentation of the supercontinent Kenorland lead to arrested orogenesis on the southern margin of the Superior province? Geoscience Frontiers, 6, 410-435, https://doi.org/10.1016/j.gsf.2014.04.003

109. Stephen R, Malinverno A. 2018 Proterozoic Milankovitch cycles and the history of the solar system. Proceedings of the National Academy of Sciences 115, 6363-6368, https://doi.org/10.1073/pnas.1717689115

110. Marov M. 2018 The formation and evolution of the Solar System. In Oxford Research Encyclopedia of Planetary Science. Oxford University Press, https://doi.org/10.1093/acrefore/9780190647926.013.2

111. Kane SR, Arney GN, Byrne PK, Dalba PA, Desch SJ, Horner J, et al. 2021 The fundamental connections between the Solar System and exoplanetary science. JGR Planets 126, e2020JE006643, https://doi.org/10.1029/2020JE006643

112. Marov MY, Ipatov SI. 2023 Migration processes in the Solar System and their role in the evolution of the Earth and planets. Physics–Uspekhi, 66, 2-31, https://doi.org/10.3367/UFNe.2021.08.039044

113. Grinin LE. 2017 Evolution of the Early Solar System in Terms of Big History and Universal Evolution. Journal of Big History, 2, 15–26, https://doi.org/10.22339/jbh.v2i1.2252

114. Blanc M, Charnoz S, Morbidelli A, Crida A, Dones L. 2025 The formation of Saturn's regular satellites: From circumplanetary disk to orbital architecture. Space Science Reviews, 221, Article 56. https://doi.org/10.1007/s11214-025-01156-8

115. Rabago I, Steffen JH. 2019 Survivability of Moon Systems Around Ejected Gas Giants. Monthly Notices of the Royal Astronomical Society 489, 2323–2329, https://doi.org/10.1093/mnras/sty2552

116. Taylor AG, Steckloff JK, Seligman DZ, Farnocchia D, Dones L, Vokrouhlický D. et al. 2024 The dynamical origins of the dark comets and a proposed evolutionary track. Icarus 420, 116207, https://doi.org/10.1016/j.icarus.2024.116207

117. van der Meer DG, Stap LB, Scotese CR, Mills BJW, Sluijs A, van Hinsbergen DJJ. 2025 Phanerozoic orbital-scale glacio-eustatic variability. Earth Planet. Sci. Lett. 619, 119526, https://doi.org/10.1016/j.epsl.2025.119526

118. Barrett TJ, Bryson JFJ, Geraki K. 2025 The source of hydrogen in earth's building blocks. Icarus 436, 116588, https://doi.org/10.1016/j.icarus.2025.116588

119. Rohling EJ, Gernon TM, Heslop D, Reichart DJ, Roberts AP, Yu J. 2024 Reconciling the Apparent Discrepancy Between Cenozoic Deep-Sea Temperatures From Proxies and From Benthic Oxygen Isotope Deconvolution. Paleoceanography and Paleoclimatology 39, e2024PA004872, https://doi.org/10.1029/2024PA004872

120. Way MJ, Del Genio AD, Kiang NY, Sohl LE, Grinspoon DH, Aleinov I, et al. 2016 Was Venus the first habitable world of our solar system? Geophysical Research Letters, 43, 8376-8383, https://doi.org/10.1002/2016GL069790

121. Strom RG, Schaber GG, Dawson DD. 1994 The Global Resurfacing of Venus. Journal of Geophysical Research: Planets, 99, 10899–10926, https://doi.org/10.1029/94JE00388

122. Schaber GG, Strom RG, Moore HJ, et al. 1992 Geology and Distribution of Impact Craters on Venus: What Are They Telling Us? Journal of Geophysical Research: Planets, 97, 13257–13301, https://doi.org/10.1029/92JE01246

123. Correia ACM, Laskar J. 2001 The four final rotation states of Venus. Nature 411, 767–770, https://doi.org/10.1038/35081000

124. Dias JA, Machado P, Robert S, Erwin J, Lefèvre M, Wilson CF, et al. 2025 Volcanic gas plumes' effect on the spectrum of Venus. Icarus 438, 116589, https://doi.org/10.1016/j.icarus.2025.116589

125. Valantinas A, Mustard JF, Chevrier V, Mangold N, Bishop JL, Pommerol A, et al. 2025 The detection of ferrihydrite in Martian red dust records ancient cold and wet conditions on Mars. Nature Communications, 16, 1712, https://doi.org/10.1038/s41467-025-56970-z

Eliminado

120. Farnsworth A, Eunice Lo YT, Valdes PJ, Buzan JR, Mills BJW, Merdith AS, et al. 2023 Climate extremes likely to drive land mammal extinction during next supercontinent assembly. Nature Geoscience 16, 901–908, https://doi.org/10.1038/s41561-023-01259-3

121. Tohver E, Schmieder M, Lana C, Mendes PST, Jourdan F, Warren L, et al. 2018 End-Permian impactogenic earthquake and tsunami deposits in the intracratonic Paraná Basin of Brazil. GSA Bulletin 130, 1099–1120, https://doi.org/10.1130/B31626.1